Catalysis Today 429 (2024) 114462

Contents lists available at ScienceDirect

Catalysis Today

journal homepage: www.elsevier.com/locate/cattod

Chemically activated hydrochars as catalysts for the treatment of HTC liquor by catalytic wet air oxidation

A. de Mora [a], J.L. Diaz de Tuesta [a], M.I. Pariente [a], Y. Segura [a], D. Puyol [a], E. Castillo [b], K. Lissitsyna [c], J.A. Melero [a], F. Martínez [a,*]

[a] Chemical and Environmental Engineering Group, ESCET, Universidad Rey Juan Carlos, c/Tulipán s/n, 28933 Móstoles, Spain
[b] Industrial Transformation Tech Unit, Repsol Technology Lab, 28935 Móstoles, Spain
[c] Formulation and Fluids Unit, Repsol Technology Lab, 28935 Móstoles, Spain

ARTICLE INFO

Keywords:
Hydrothermal carbonization
Wet air oxidation
Activated hydrochar
Biochemical methane potential

ABSTRACT

Hydrothermal carbonization (HTC) is a highly efficient and valuable technology for treating wet solid wastes and producing solid carbon-based materials named hydrochar. In this work, a hydrochar coming from the HTC of an anaerobic digestion sludge of wastewater treatment plant was used to assess the influence of several activation agents, a base (KOH) and different chloride salts ($FeCl_3$, $ZnCl_2$, and $CuCl_2$) with the exact molar quantities, to develop materials with enhanced surface area and potential inclusion of metal active species for application in wet air oxidation processes. The KOH as an activating agent increased the surface area of hydrochar up to ca. 1000 m^2/g of BET surface area. The employment of $CuCl_2$ and $FeCl_3$ as activating agents allows Cu- and Fe-rich doped materials of remarkable surface areas with 49.1 and 42.5 wt% of each metal, respectively. Likewise, the catalytic behavior of the different synthesized carbon-based materials as metal-free and metal-doped catalysts was evaluated for the Catalytic Wet Air Oxidation (CWAO) of a HTC aqueous liquor from a HTC process of animal manure to produce a valuable stream of higher biochemical methane potential in anaerobic digestion. CWAO effluents increased the proportion of carboxylic acids as final by-products due to the oxidation of more complex organic compounds of the initial effluent (ketones, phenols, aromatics and olefins). The CWAO treatments improve the anaerobic digestion rate in biochemical methane potential tests, although the methane production was limited by the lower TOC concentration of the treated streams after CWAO. This research contributes to developing sustainable and efficient strategies for the HTC-liquor treatment, using its solid hydrochar as catalysts, closing the loop of a Circular Economy.

1. Introduction

Hydrothermal carbonization (HTC) is an eco-friendly, flexible and highly efficient technology typically used to treat wet solid wastes [1,2]. Hydrochar, the primary solid product of hydrothermal carbonization (HTC), is considered a waste-to-char product. Its structure is like natural lignite, characterized by its high energy density, low levels of sulfur and chlorine, and high carbon content. However, hydrochar obtained through HTC often exhibits a small surface area and porosity, limiting its potential for other applications, such as adsorbents or catalysts [2]. To overcome those limitations, it is necessary to enhance the existing pores by developing new pores to improve the quality of the raw hydrochar. The main activation methods include both chemical and physical processes [1]. Chemical activation agents, such as inorganic acids, bases, or salts, have produced activated carbon materials with high specific surface areas and surface oxygenated functional groups using mild temperatures and short activation times [1,3]. However, a notable novelty in this field lies in the scarcity of studies that systematically compare activation processes using the same quantity of activating agents, making comparisons challenging and labor-intensive. Furthermore, it underscores the importance of metal incorporation in the activation process, which could enhance the catalytic properties of the resulting material [1].

On the other hand, because of the HTC process, a liquid fraction is produced. Depending on the HTC operating conditions, the HTC liquor can contain up to 15–20% of the initial carbon, primarily as formic and acetic acids, sugars, nutrients, and other compounds [4]. This leads to chemical oxygen demand (COD), ranging from 2 to 70 g/L [5].

* Correspondence to: Chemical and Environmental Engineering Group, Universidad Rey Juan Carlos, Móstoles, Spain.
E-mail address: fernando.castillejo@urjc.es (F. Martínez).

https://doi.org/10.1016/j.cattod.2023.114462
Received 15 July 2023; Received in revised form 3 November 2023; Accepted 16 November 2023
Available online 22 November 2023

However, recalcitrant or inhibitory compounds such as alcohols, ketones, phenols, and cyclic oxygenates (furans) are also generated during the HTC process [6]. Cyclic hydrocarbons, including derivates of benzene and polycyclic aromatic hydrocarbons, are often present, posing potential ecological hazards if left untreated [7]. Furthermore, certain nitrogen compounds may be toxic, such as indole, pyrrole derivatives, amino phenol compounds and pyrazine, which can be detrimental to microorganisms in a conventional wastewater treatment plant [8]. Consequently, using microalgae or anaerobic digestion to treat HTC effluents results in inefficiency since toxic compounds in the aqueous phase inhibit these processes [4].

The toxicity of the HTC liquor was examined by Czerwińska et al. for agriculture purposes, who consider its use as a potential fertilizer. Plants were exposed to HTC liquor for seven days, revealing that the liquid's toxicity was at 100%. To mitigate this toxicity, the HTC solution had to be diluted at least 100-fold [9]. Moreover, it has been demonstrated that when this effluent is directly discharged into the environment, it contributes to 100% freshwater eutrophication and a 90% freshwater eco-toxicity potential factor due to the release of nutrients and harmful metals [10]. Consequently, the liquid fraction derived from HTC represents a significant challenge that hinders the progress of HTC technology [7,11].

Before treating the liquor, many studies have studied its recirculation to the HTC process, which results in a final HTC liquor with a higher organic matter [12]. More innovative solutions propose its valorization through advanced oxidation processes [13–15]. One attractive alternative is the wet air oxidation (WAO) process. WAO involves a process conducted at high temperatures (200–320 °C) and pressure (20–200 bar) while introducing an excess of air or oxygen in the reactor [16]. While wet oxidation has been successfully applied to sewage sludge and several industrial wastewater streams, there have been relatively few studies on its application for treating the liquid phase resulting from hydrothermal carbonization [6,17]. Using metal catalysts to decrease the temperature and pressure operation conditions in this process has also been explored. Thus, catalytic wet air oxidation (CWAO) has been proven to be a promising alternative, mainly when operating under mild conditions using effective catalysts [18].

Cost-effective and stable solid catalysts that avoid metallic sludge streams after subsequent separation steps when using dissolved metal salts are one of the main challenges for industrial implementation [19]. Transition metal-based catalysts such as iron, manganese, cobalt, and copper have exhibited significant activity in degrading organic pollutants [20,21]. During the process of CWAO, catalytic active sites produce active oxygen species from O_2 that gradually convert organic pollutants into shortened oxidized organic compounds, CO_2 and H_2O [22]. Moreover, the leaching of transition metals as active components during reactions is also a serious issue that must be addressed [21]. Metal-free activated carbon materials (AC) synthesized without transition metals also offer a promising alternative for CWAO processes in wastewater treatments. The absence of metals in the carbon-based catalysts eliminates concerns regarding leaching and subsequent post-treatment requirements often associated with metal-containing catalysts [23].

The novelty of this work is focused on: i) the study of the effectiveness of different agents (KOH base and chloride salts like $FeCl_3$, $ZnCl_2$, and $CuCl_2$ using the exact molar concentration) for the activation of hydrochar materials (increased porosity and metal doping); and ii) the catalytic performance of metal-free activated carbon (AC) and doped-AC catalysts in the catalytic wet air oxidation of the HTC aqueous liquor to produce more biodegradable streams for anaerobic digestion with higher biochemical methane potential. The results of this work expand the potential use of the HTC solid hydrochar product as catalysts and offer solutions for the valorization of the HTC aqueous liquor through catalytic wet air oxidation processes.

2. Materials and methods

2.1. Origin of hydrochar and HTC aqueous liquor

The hydrochar and the HTC aqueous liquor used in this work were provided by Ingelia using two different feedstocks in the HTC process: i) the slurry of an anaerobic digester of a wastewater treatment plant for the hydrochar and ii) the animal manure for the aqueous liquor. In both cases, the operation conditions of the HTC process were 200 °C, 20 bar and 4 h of operation. The aqueous liquor was collected and stored at 4 °C to prevent alterations in their composition.

The HTC aqueous liquor was exhaustively characterized. The pH was monitored using a GLP-22 digital pH meter (HACH LANGE SPAIN, S.L. U). Chemical Oxygen Demand (COD), Total Solids (TS), Volatile Total Solids (VTS) and Total Suspended Solids (TSS) were measured following APHA-AWWA Standard Methods 5220. D, 2540. B, 2540. E and 2540. D, respectively. Total Kjeldahl Nitrogen (TKN) was measured using a Vapodest 450 (Gerhardt, Analytical Systems) for the digestion of the samples, following APHA-AWWA Standard Method 4500-Norg C. NH_4^+ and PO_4^{3-} were determined using a Smartchem 140 (AMS Alliance), following APHA–AWWA Standard Methods 4500-NO_2 B and 4500-P E, respectively.

2.2. Synthesis and characterization of the activated hydrochar materials

Activating agents $FeCl_3$ (98%), $ZnCl_2$ (98%), $CuCl_2$ (99%) and KOH (85%) were purchased from Scharlab, Across Organic and Labkem. HCl (35–38%) and H_2SO_4 (98%) for materials washing were both from Labkem.

The modified hydrochar was all obtained via solid mixing of the four activating agents with the hydrochar (HC sample). 1 g of hydrochar (HC) was mixed with 6 mmol of $FeCl_3$, $ZnCl_2$, $CuCl_2$ or KOH, similar to previous work [24]. Later, the hydrochar materials were thermally activated through a modified method described elsewhere [25] in a tubular furnace ST-115020-PAD P (Forns Hobersal S.L) equipped with quartz tubes and a maximum working temperature of 1150 °C. The synthesis protocol involves a carbonization step at 420 °C for 30 min in a flow N_2 atmosphere (heating rate of 4 °C/min), an activation step (850 °C for 80 min) in a flow N_2 atmosphere with a 4 °C/min of heating rate. Finally, the materials were washed with HCl 0.2 M and water up to neutral pH in the rising water and dried at 100 °C overnight. To decrease the ashes content and, thus, increase the specific surface area, the KOH-modified hydrochar was washed with H_2SO_4 (50%) at 150 °C for 3 h. The hydrochars activated with KOH, $FeCl_3$, $ZnCl_2$, $CuCl_2$ were labelled as K-AC, $FeCl_3$-AC, $ZnCl_2$–AC and $CuCl_2$–AC, respectively. The hydrochar activated with KOH and further washed with sulfuric acid was labeled K–SA–AC. For a comparative purpose, HC was also treated with sulfuric acid and subsequent thermal activation using the abovementioned method, resulting in an SA–AC sample. An additional pyrochar (PC) was also prepared using the same thermal treatment without an activating agent.

The synthesized carbon materials were characterized according to the following techniques. Thermogravimetric Analysis (TGA) was performed on a simultaneous TGA-DSC thermobalance (TGA-DCS1, Mettler-Toledo, S.A.E.) using a flow rate of 100 mL/min of nitrogen and a heating rate of 10 °C/min. Moisture, volatile matter and ashes were determined from TGA. Moisture and volatile matter were resolved as weight loss up to 105 °C and 900 °C at inert atmosphere, whereas ashes content was calculated as the final percentage weight of samples at 900 °C at oxidant atmosphere. Finally, fixed carbon was determined as 100-moisture (%) - volatile matter (%) – ashes (%). The elemental analysis (CHNS) was carried out in a Flash 2000 analyzer (Thermo Fisher Scientific, Massachusetts, USA), provided with a thermal conductivity detector (TCD). The oxygen content was calculated by difference, considering the ash and moisture content in the solid samples - O (wt%) = 100 – C (wt%) – N (wt%) – S (wt%) – H (wt%) – ashes content (wt%)-.

The metal content of the activated hydrochars was determined by ICP-OES using Vista AX Pro-720ES equipment. The samples were previously digested under a strong acid medium (HNO_3/HCl).

Nitrogen adsorption isotherms at 77 K were carried out using a Micro Active Tristar II Plus (Micromeritics). The samples were outgassed using a heating rate of 5 ºC/min until 90 ºC for 30 min and then by another heating rate of 5 ºC/min until 150 ºC for 480 min. The specific surface area was calculated by Brunauer-Emmett-Teller (S_{BET}) and Langmuir ($S_{Langmuir}$) methods [26]. The external surface area (S_{ext}) and the micropore volume (V_{mic}) were obtained by the *t*-method (thickness was calculated by employing ASTM standard D-6556–01), as detailed in previous works [27,28]. The microporous surface area (S_{mic}) was determined as the subtraction of S_{ext} from S_{BET}. The total pore volume (V_T) was defined as the net amount of nitrogen adsorbed to the $p/p^o = 0.99$.

X-ray photoelectron spectroscopy (XPS) measurements were performed on a Physical Electronics Spectrometer (PHI 5700, Lake Drive East, Chanhassen, MN, USA) with X-ray MgKα radiation (15 kV, 300 W and 1253.6 eV) as the excitation source to analyze the surface chemistry of each catalyst.

2.3. Catalytic wet air oxidation of HTC liquor and analytical techniques

CWAO experiments were performed in a 500 mL T316 stainless steel autoclave reactor, resistant to high pressures and temperatures: model 4575 A manufactured by Parr Instrument Company, USA [29]. Typically, 200 mL of the HTC liquor and 2.4 g/L of activated carbon catalyst are placed in the reactor. The catalyst dose was selected considering the revised literature for treating high-loaded industrial wastewater in which the TOC/[catalyst] ratio was around 1 [29–31]. The pH of the wastewater (7.8 ± 0.1) was not modified and adjusted before or during the treatment. Initially, nitrogen gas flow was passed through the headspace of the reaction vessel to ensure inert conditions and continuous stirring was fixed at 400 rpm. Then, the air was supplied up to 50 bar to maintain the wastewater in the liquid phase. Finally, the reactor was heated to the operating temperature (250 ºC), reaching ca. 115 bar of total pressure. Once the reactor was heated at the desired temperature, which took 60 min, samples were withdrawn after 0, 60, 90, 120 and 180 min, cooled, filtered, and immediately analyzed.

TOC (Total Organic Carbon) concentration was determined in a combustion/non-dispersive infrared gas analyzer (TOC-L Shimadzu). Furthermore, the pH of the solution was measured using a GLP-22 digital pH meter (HACH LANGE SPAIN, S.L.U). The metal content in the filtered solution after the reaction was measured by ICP-OES analysis in a Varian Vista AX spectrometer to determine the metal leaching in the effluent.

GC×GC-TOFMS analyses were performed on Pegasus4D (Leco, St. Joseph, MI) with an Agilent Technologies 7890 gas chromatograph (Palo Alto, CA) equipped with a second oven and a cryogenic modulator. The GC column combination consisted of a MegaWax-1 (30 m length; 0.25 mm inner diameter; 0.25 μm film thickness) and a ZB-50 in the second oven (1,5 m length; 0.1 mm inner diameter; 0.1 μm film thickness).

Color number (CN) was evaluated following the methodology reported in the literature [32,33]. Firstly, spectral absorption coefficient (SAC_i) was determined by absorption (Abs_i) at 436, 525 and 620 nm wavelengths as $SAC_i\,(m^{-1}) = Abs_i\,/x$, where x refers to the path length of the cuvette used in measurements (0.01 m). Then CN was determined from each SAC_i as detailed in Eq. (1):

$$CN(m^{-1}) = \frac{SAC_{436}^2 + SAC_{525}^2 + SAC_{620}^2}{SAC_{436} + SAC_{525} + SAC_{620}} \quad (1)$$

2.4. Biochemical methane potential (BMP) tests

Anaerobic digestibility of the remnant fraction upon the thermochemical experiments was explored through standard BMP tests. The anaerobic inoculum was sourced from an expanded granular sludge bed reactor treating brewery wastewater in Guadalajara, Spain. The experiments were performed in triplicate in 160 mL serum bottles inoculated with 1.5 gVS/L of anaerobic granular sludge. After the thermal treatments, the bottles were filled with 16.67 mL of the remnant liquid fractions. A source of macro and micronutrients was added, as per Puyol et al. [34]. A source of alkalinity was added at 1 g $NaHCO_3$/L. The bottles were filled with Milli-Q water up to 100 mL. The bottles were closed with a rubber stopper and sealed with aluminum crimps before flushing with N_2 to achieve anaerobic conditions. Then, the bottles were incubated statically in a 37 ºC-controlled incubator for 20 d. Negative control was also performed in triplicate, where no liquid substrate was added. The negative control was used to subtract the amount of methane produced by the self-digestion of the granular sludge. A positive control was also included, where 4 gCOD/L (1.327 gC/L) of a mixture of acetic, propionic, and butyric acids was used as substrate at a 1:1:1 COD ratio. The positive control was used to estimate the specific methanogenic activity of the granular sludge. The methane production was measured by checking the gas pressure daily and extracting 8 mL of gas samples twice weekly. The samples were injected into a gas chromatograph with a thermal conductivity detector (Agilent 7820 A GC, Santa Clara, CA, USA). More details about the method are provided elsewhere [35]. Liquid samples were extracted at the end of the experiment to analyze the soluble TOC, thereby calculating the TOC consumption over the BMP tests.

Kinetic parameters of the anaerobic digestion were estimated by fitting the experimental data of mL CH_4/gTOC to a first-order model as [36], thus calculating the first-order hydrolysis rate (kH, in 1/d) and the BMP (B_0, in mL CH_4/gTOC). Parameter uncertainty was determined using two-tailed t-tests calculated from the standard error in the parameter value obtained from the Fisher information matrix. The parameter uncertainty surface (with k_H, B_0, J = Jcrit, 5% significance threshold) has also been assessed as described in [37]. Confidence intervals (at 95%) were also calculated based on two-tailed t-tests from the parameter standard error, as above, and used for statistical representative comparisons. All the statistical analyses of BMP tests were performed by using Aquasim 2.1d.

3. Results and discussion

3.1. Catalyst thermal stability

The raw hydrochar (HC sample) and the prepared activated carbons (ACs) were analysed by TGA in air and nitrogen atmosphere at 10 ºC/min to compare each other and obtain their proximate analyses. Weight loss profiles as a function of the temperature are depicted in Fig. 1. At air atmosphere, activated hydrochar materials prepared using copper, zinc and iron chlorides present a significant weight loss around 540 ºC reaching values of 25.0, 27.3 and 49.1 wt% for $CuCl_2$–AC, $FeCl_3$–AC, $ZnCl_2$–AC, respectively (Fig. 1.a and e). This denoted a high oxidation resistance, only 100 ºC less than ordered structured carbon-based materials such as graphite or carbon nanotubes [38]. The slope of the curve profile among chloride-salt activated materials directly depends on the quantity loss since the fastest losses were found for $ZnCl_2$–AC material (up to −0.82 wt%/ºC), followed by $FeCl_3$–AC (−0.20 wt%/ºC) and $CuCl_2$–AC (−0.08 wt%/ºC). Non-activated materials (pyrochar and sulfuric acid treated hydrochars) also show a weight loss starting at 400 ºC with similar slope curve profiles between them (−0.28 and −0.26 wt %/ºC for PC and SA–AC, respectively) (Fig. 1b and d). However, constant mass losses were kept longer than chloride-activated materials, reaching 35.4 and 72.4 wt% for PC and SA–AC weight loss, respectively. Potassium-activated materials (K–AC and K–SA–AC) show lower thermal stability than previous materials since they also present one primary mass loss at a lower temperature, 300 ºC (Fig. 1.b and f). The highest mass loss is at 441 ºC (−0.24 wt%/ºC) and 477 ºC (−0.89 wt%/ºC) for

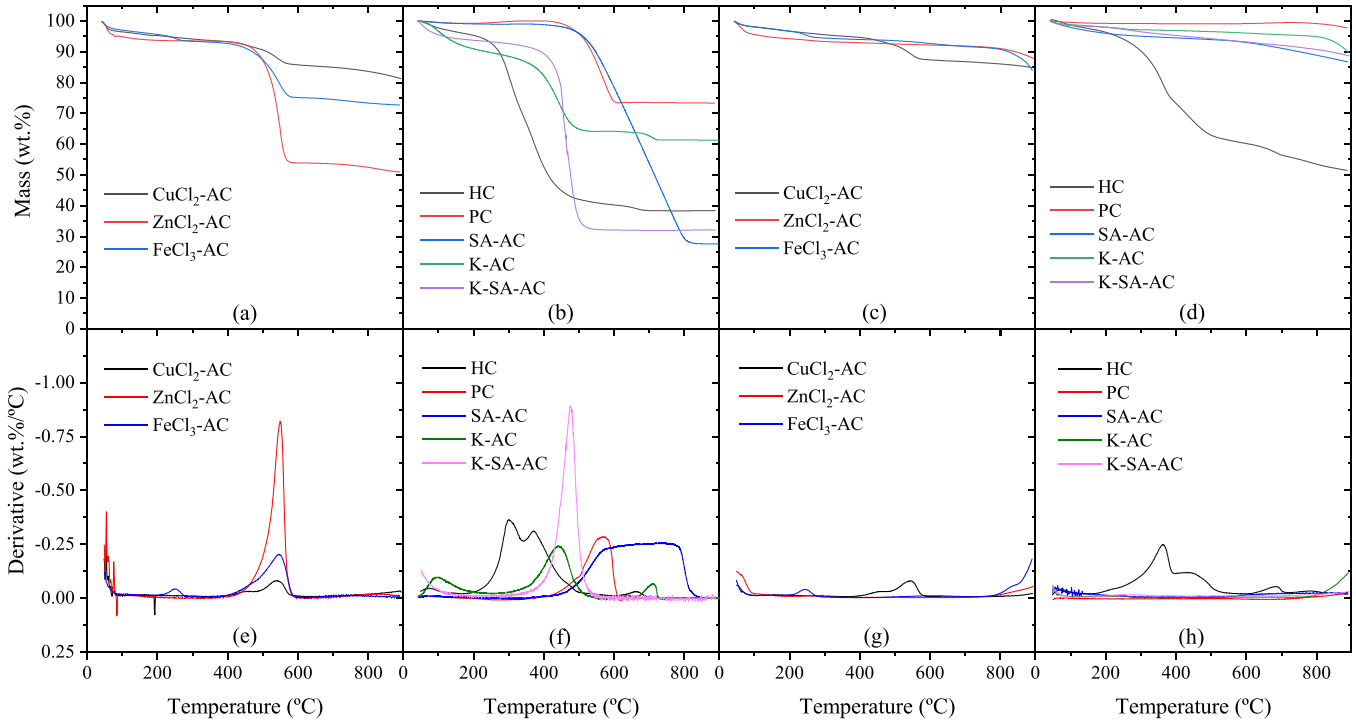

Fig. 1. Thermogravimetric analysis in air (a-b) and nitrogen atmosphere (c-d); and signal derivative (e-f, g-h, respectively) of metal chloride precursors and raw and activated hydrochar materials.

K–AC and K–SA–AC, respectively. As expected, the lowest thermal stability is found for raw precursor (HC sample), which shows mass losses from ca. 200 °C to 500 °C. In that range, two main peaks are located at 299.2 °C and 371.7 °C, likely due to two main components in the matrix of the hydrochar produced from the digestate obtained in the anaerobic wastewater treatment plant digester. In biomass feedstock, even hydrochars prepared at low temperatures, similar peaks are observed and associated with the cellulose and hemicellulose components of the biomass [1,39].

The thermogravimetric analyses of the catalysts at inert conditions show that materials are highly stable, as expected, considering they all were prepared up to 850 °C. Only the HC raw precursors show significant mass losses in a similar range of temperatures than those observed in oxidant conditions (from ca. 200 °C to 500 °C) (Fig. 1.d and h).

Table 1 summarizes the proximate analysis obtained from TGA results for each catalyst prepared. The moisture content of the materials is due to the water ambient adsorbed during the short time of their preparation since they were dried previously at 105 °C overnight. The volatile contents of the ACs do not show significant differences, taking values from 10.3 to 16.1 wt% for ACs. As expected, HC raw precursor presents a higher content value since it was stabilised at 200 °C. The ash content of materials takes the highest values and gives the following order: $CuCl_2$–AC (75.1 wt%) > $FeCl_3$–AC (72.7 wt%) > PC (66.7 wt%) > K–AC (61.2 wt%) > $ZnCl_2$–AC (50.9 wt%) > HC (38.4 wt%) > K–SA–AC (32.1 wt%) > SA–AC (27.6 wt%). As observed, acid-treated materials show the lowest ash content, even lower than raw HC precursor, likely due to the washing of metals by acid attack, as observed in previous works [40,41]. The fact that PC presents higher ashes content than raw precursor is also typically found in literature since volatile content is released during thermal treatment and inorganic matter is concentrated in the resulting material. The highest quantities of ash contents were found for $CuCl_2$–AC and $FeCl_3$–AC, which may be ascribed to partial loads of copper and iron on the surface of the materials.

Table 1
Proximate analysis of activated hydrochars.

Catalyst	Moisture content (wt%)	Volatile matter (wt%)	Ash content (wt%)	Fixed carbon* (wt%)
$CuCl_2$–AC	2.8	15.2	75.1	6.9
$ZnCl_2$–AC	4.9	12.2	50.9	31.9
$FeCl_3$–AC	2.6	16.1	72.7	8.6
K–AC	2.5	10.3	61.2	25.9
K–SA–AC	3.1	11.4	32.1	53.4
SA–AC	1.4	13.3	27.6	57.7
PC	0.6	2.3	66.7	30.4
HC	2.0	48.6	38.4	11.1

* Fixed carbon = 100 – moisture (%) – volatile matter (%) – ashes (%)

When biomass is used as feedstock, ash content takes values lower than those observed for the materials in this work. However, catalysts prepared from solid wastes used to have a more complex matrix and inorganic content are highlighted. In previous reports, thermal and activation methods of matured compost obtained from municipal solid wastes lead to up to 81.5 wt% of ashes in some materials [40,41]. The fixed carbon of the catalysts takes the following order: SA–AC (57.7 wt%) > K–SA–AC (53.4 wt%) > $ZnCl_2$–AC (31.9 wt%) > PC (30.4 wt%) > K–AC (25.9 wt%) > HC (11.1 wt%) > $FeCl_3$–AC (8.6 wt%) > $CuCl_2$–AC (6.9 wt%). As observed, acid-treated materials show the highest quantity of fixed carbon due to both the release of volatile content and the leaching of metal species, leading to obtained C-rich materials. Surprisingly, $FeCl_3$–AC and $CuCl_2$–AC present lower contents than HC raw precursor, likely due to a higher release of organic content during the activation process and the dope of the materials with the copper or iron metals.

3.2. Catalyst composition

The catalyst composition was determined through CHNS-elemental analysis and ICP-OES (Table 2). As observed, C-content takes values close to those obtained for fixed carbon. Notably, all materials show higher values of C than fixed carbon, likely due to the volatile content of materials compromised volatile organic compounds. Only two materials present a value of C content lower than those observed for fixed carbon,

Table 2
Results of the ultimate analysis (CHNS elemental analysis) and ICP-OES.

Catalyst	C (wt%	H (wt%)	N (wt%)	C/H (wt./wt.)	O* (wt%)	Cu (wt%)	Zn (wt%)	Fe (wt%)	K (wt%)
$CuCl_2$–AC	22.1 ± 0.3	0.39 ± 0.01	0.53 ± 0.02	58.2	1.2	49 ± 3	0.2 ± 0.1	4.7 ± 0.3	0.41 ± 0.05
$ZnCl_2$–AC	38.3 ± 0.2	0.81 ± 0.08	0.6 ± 0.1	47.3	8.0	< DL	0.50 ± 0.05	6.1 ± 0.2	0.42 ± 0.01
$FeCl_3$–AC	18.2 ± 0.3	0.28 ± 0.01	0.9 ± 0.1	65.0	7.5	< DL	< DL	**43** ± 2	0.33 ± 0.05
K–AC	29 ± 3	1.4 ± 0.1	0.12 ± 0.06	20.7	8.2	< DL	< DL	11.1 ± 0.5	**5.6 ± 0.2**
K–SA–AC	52.0 ± 0.1	0.72 ± 0.08	0.39 ± 0.09	72.2	14.8	< DL	< DL	0.1 ± 0.1	0.5
SA–AC	46.3 ± 0.2	1.20 ± 0.1	0.22 ± 0.07	38.6	23.0	-	-	-	-
PC	31.5 ± 0.3	0.63 ± 0.02	0.19 ± 0.02	50.0	2.1	0.02	< DL	11.5 ± 0.6	0.74 ± 0.05
HC	37.2 ± 0.3	2.32 ± 0.02	4.41 ± 0.04	16.0	17.0	< DL	< DL	4.4 ± 0.4	0.35 ± 0.07

* Oxygen content was determined as O (wt%) = 100 – C (wt%) – N (wt%) – S (wt%) – H (wt%) – ashes content (wt%).

and those are the acid-treated materials (53.4 and 57.7 wt% of fixed carbon, whereas C-content is 52.0 and 46.3 wt% for K–SA–AC and SA–AC, respectively) (*see* Fig. S1 for more details). This may be ascribed to the fact that surface oxygen groups may be released during thermal treatment, so the volatile matter of those catalysts is not carbon volatile matter. The H and N content of pyrolyzed materials reached values up to 1.7 wt%, with no significant differences among the treatments performed. The hydrogen and nitrogen content of HC raw precursor is higher than the thermally treated materials, likely due to the release of H and N-rich volatile matter during the treatments. Accordingly, the C/H (wt./wt.) ratio increases from 16.0 for the HC sample to 72.7 due to the carbonization process, with a predominance of dehydration and aromatization reactions [42]. In a previous work dealing with the HTC of compost and further pyrolysis [32], it was observed that the pyrochar had a lower carbon-to-hydrogen ratio (by weight) and a higher concentration of ashes compared to the PC sample. This demonstrates that the carbon source used in this research enables the preparation of more carbon-rich materials, as indicated by their higher fixed carbon content.

The organic oxygen content of the materials takes values from 1.2 to 23.0 wt%. The highest values were found for acid-treated materials (14.8 and 23.0 wt% for K–SA–AC and SA–AC, respectively) due to the acid attack likely generating functional oxygen groups that agree with the difference between fixed carbon and carbon content determined for these materials. The oxygen content for the non-acid treated materials ranges from 1.2 to 8.2 wt%, which is lower than the O-content of HC raw precursor, as expected considering the oxygen released during thermal treatments.

ICP-OES analysis of the acid-digested samples allows to determine the metal content of the catalysts. As observed, using $CuCl_2$ and $FeCl_3$ as activating agents to develop porosity also allows a metal-doped material rich in each metal. At the abovementioned conditions, the activation with $CuCl_2$ and $FeCl_3$ of the HC raw precursor led to a catalyst with 49.1 and 42.5 wt% of copper and iron, respectively. However, using $ZnCl_2$ as an activating agent does not allow activating and doping of the HC raw precursor since 0.5 wt% of Zn content was obtained. The lower evaporation temperature of metallic zinc compared to metallic copper and iron is likely the reason for the complete disappearance of zinc in the $ZnCl_2$-AC sample [43]. The activation with KOH leads to slightly incorporating potassium on the resultant material (5.6 wt% of K in K–AC sample), which is removed whether acid treatment is conducted (0.5 wt % of K was observed for K–SA–AC catalyst). Even the iron content of HC precursor (4.4 wt%) decreases with the acid treatment (0.1 wt% K–SA–AC). If an acid treatment is not conducted, iron is concentrated due to the release of volatile matter during pyrolysis from 4.4 wt% for the HC sample to 4.7–11.5 wt% for non-iron activated samples. In brief, it can be concluded that using metal species as activating agents may lead to developing textural properties and dope materials with specified attractive metals for a catalytic process.

3.3. Burn-off and textural properties

Table 3 summarizes the burn-off observed during thermal treatments coupled with textural properties. BET, Langmuir, microporous and external surface area, micropore, and total pore volume. As follows, the burn-off obtained during the preparation of materials takes values from 14.8 wt% to 84.4 wt%. The lowest values were observed for materials activated with chloride agents (14.8, 25.3 and 39.7 wt% for $CuCl_2$–AC, $FeCl_3$–AC, and $ZnCl_2$–AC) and higher mass losses during pyrolysis were observed for SA–AC (58.3 wt%) > K–AC (64.4 wt%) > K–SA–AC (84.4 wt%). The development of porosity followed a similar trend that mass losses, as depicted in Fig. S2. Accordingly, the highest surface areas and pore volume were obtained for K–SA–AC catalyst (S_{BET} = 997 m^2/g, $S_{Langmuir}$ = 2440 m^2/g, S_{ext} = 532 m^2/g, and V_T = 0.913 cm^3/g). However, the highest micropore development was achieved using $ZnCl_2$ as an activating agent, reaching 588 m^2/g of micropore surface area and 86% of micropore volume (determined as V_{mic}/V_T·100).

Table 3
Textural properties of activated hydrochars.

Catalyst	Burn-off (wt%)	S_{BET} (m^2/g)	$S_{Langmuir}$ (m^2/g)	S_{mic} (m^2/g)	S_{ext} (m^2/g)	V_{mic} (cm^3/g)	V_T (cm^3/g)
$CuCl_2$–AC	14.8	112	192	96	16	0.05	0.07
$ZnCl_2$–AC	39.7	670	985	588	82	0.303	0.349
$FeCl_3$–AC	25.3	277	676	143	134	0.076	0.25
K–AC	64.4	448	949	249	199	0.131	0.353
K–SA–AC	84.4	997	2440	465	532	0.238	0.913
SA–AC	58.3	66	117	48	18	0.025	0.042
PC	51.9	65	285	8	57	0.003	0.09
HC	-	15	< LD	< LD	< LD	< LD	< LD

The relationship between textural properties and burn-off is well-known [44,45], as demonstrated in Fig.S2 for the materials prepared in this work. However, a closer relationship was found between the BET surface area and the ashes' content among these materials (Fig. 2.) Plotted data shows that the lower the ashes content, the higher the BET

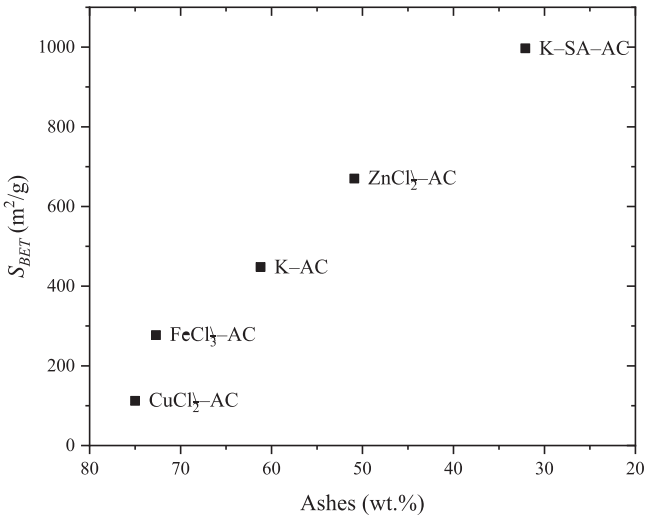

Fig. 2. BET surface area as a function of ashes content of the catalysts.

surface area; in other words, BET surface area increases when ashes content decreases. This means that the porosity of these materials comes from their organic part (the C-rich matrix), whereas there is no significant contribution to porosity from inorganic matter.

3.4. Surface chemistry

The XPS technique explored the elemental content and functional surface groups of the catalysts, and the deconvolution of the peaks was obtained in the analyses. Table 4 summarizes the O/C atomic ratio of each prepared material according to XPS analysis. As observed, oxygen (both organic and inorganic) per atom of carbon takes the highest values for potassium-activated materials (0.66 at/at for both K–AC and K–SA–AC), whereas the lowest value was observed for $FeCl_3$–AC (0.14 at/at). Among chloride-activated carbon materials, significant differences were observed among them: $CuCl_2$–AC (0.59) > $ZnCl_2$–AC (0.49) > $FeCl_3$–AC (0.14), that was precisely the opposite difference for organic oxygen per carbon determined by CHNS-elemental analysis: $CuCl_2$–AC (0.06) < $ZnCl_2$–AC (0.21) < $FeCl_3$–AC (0.41). This means that the oxygen surface content of CuCl2–AC due to the inorganic content (copper oxides) on the surface of materials is considerably higher than the oxygen in the other materials.

The nature of the surface oxygen groups on the materials was determined by deconvolution of the O1s region spectra obtained by XPS. For that purpose, 7 peaks were considered and associated with metal oxides and other organic functionalities, following the literature [24,46–48]. Considered peaks were O1: Fe_3O_4, CuO, ZnO (529.7 eV), O2: Fe_2O_3, FeO, CuO (530 eV), O3: C═O, metal hydroxides, alumina and carbonates (531.2 eV), O4: hydroxyls, ethers and C–O in esters, amides, anhydrides (532.3 eV), O5: C–O in esters and anhydrides (533.3 eV), O6: carboxylic groups (534.2 eV), and O7-water (536.1 eV). More details can be found in Table S1. The peaks obtained, coupled with the relative areas of each one and the cumulative fit peak, are depicted in Fig. 3.

As observed, chloride-activated materials present the highest quantities of O1 and O2 (1.7–9.7% and 8.7–16.8% of relative area, respectively) due to metal oxides on their surface. Most of the materials present on the surface high quantities of carbonyl and hydroxyl oxygen groups (O3 and O4 take values up to 48.6% and 35.1% of relative area, respectively), except acid-treated materials, which take the lowest values of these groups (4.1% and 15.7% of relative area of O3 and O4 for K–SA–AC material, and 10.9% and 23.6% of relative area of O3 and O4 for SA–AC, respectively). This may be ascribed to the highest contribution of O5 and O6 (carboxylic groups) on these materials (39.8% and 31.4% of relative area of O5 and O6 for K–SA–AC material, and 26.0% and 27.6% of relative area of O5 and O6 for SA–AC, respectively), which it is the highest relative area found for O5 and O6 among all materials, likely due to the acid attack conducted in the preparation of K–SA–AC and SA–AC.

Fig. 4 represents the Cu2p specter region of the $CuCl_2$–AC and the deconvolution performed according to the data available in the literature [48,49]. Briefly, Cu_2O (932 eV) and CuO (2 peaks at 933.1 and 934.6 eV) were considered. However, the Cu2p specter region is quite similar to those found for CuO materials in the literature [49,50], and Cu_2O was negligible, verifying that the copper presence on the surface of the material is CuO.

Table 4
Semiquantitative O/C atomic ratio obtained through XPS analysis.

Catalyst	O/C (at./at.)
$CuCl_2$–AC	0.59
$ZnCl_2$–AC	0.49
$FeCl_3$–AC	0.14
K–AC	0.66
K–SA–AC	0.66
SA–AC	0.23
PC	0.43
HC	0.33

3.5. Evaluation of the catalytic wet air oxidation performance of HTC effluent

The HTC aqueous liquor is an actual effluent coming from a hydrothermal carbonization process. Table 5 shows the characterization of the effluent considered in this work. It is essential to note the high organic matter content concerning the TOC and COD of this effluent. Additionally, the HTC aqueous liquor showed a low concentration of metals, a neutral pH and a very dark color due to the compounds produced during the HTC process. Moreover, it contains 2.2 g/L of TS. These characteristics classify this process stream as hazardous waste, making it challenging to handle and treat [51,52].

Wet air oxidation (WAO) has proven to be an effective process for treating wastewater with high organic matter content, allowing the total or partial degradation of toxic or refractory compounds for biological treatment [53]. Initially, operation conditions of 250 °C and 50 bar of air pressure were used for testing the catalytic performance of activated hydrochars [29]. In CWAO processes, the role of metallic species and the porosity of the carbon surface have been considered beneficial for enhancing organic removal [54]. Thus, the catalytic effect of the activating agent by equal mmol of the agent was compared, as shown in Fig. 5a. The conversion of TOC obtained with different catalysts suggests that the presence of Cu had a very positive effect rather than other metals or surface area when the catalytic activity of $CuCl_2$–AC (112 m^2/g of S_{BET}) is compared to other catalysts. In this sense, Cu is the active center of the $CuCl_2$–AC catalyst. Reza et al. studied the CWAO of HTC effluent using a CuO catalyst. They also obtained a 74% of TOC reduction [6]. However, the HTC process liquor was diluted, whereas in the present study, the HTC liquor was treated as received. Wakabayshi and Okuwaki also found powdered copper metal to be a very efficient catalyst (compared to the metal powders of nickel, chromium, manganese, and cobalt) for the high-temperature (250 °C) CWAO of sodium acetate in highly alkaline solution [55]. The reasons for the high activity of copper-based catalysts are poorly understood. The activity could be due, in part, to the tendency of copper to complex with some compounds (such as some acids) and due to copper initiating/generating free-radical intermediates that catalyze the WAO [56]. To discard the first assumption, the leaching of the copper was further determined.

The catalyst activated with other activating agents presents lower catalytic activity despite the high specific surface area (K-SA-AC) or iron content ($FeCl_3$-AC). It is shown that the $ZnCl_2$-AC catalyst is very active, although the zinc is not retained in the structure due to the acid washing. The best performance of this catalyst compared with the one activating with $FeCl_3$ could be related to the higher specific surface area (670 and 277 m^2/g of S_{BET} for $ZnCl_2$ and $FeCl_3$, respectively) and the lower O/C ratio for the $FeCl_3$ material (0.49 and 0.14 for $ZnCl_2$ and $FeCl_3$, respectively, Table 4). The influence of the textural properties of carbon materials in CWAO is well understood (pore size and surface area); however, the role of surface chemistry still needs to be fully understood [23]. The ability of carbon atoms to bind with each other in various ways to form linear, planar, and tetrahedral arrangements leads to the production of carbon materials with a wide range of properties. Most authors support the positive effect of O surface groups [57], as shown in these experiments, where the highest activity is obtained for the material with a higher O/C ratio ($CuCl_2$–AC > $ZnCl_2$–AC > $FeCl_3$–AC). Regarding the catalyst activated with KOH, the critical role of the specific surface area can be seen, as higher activity was obtained for the K-SA-AC catalyst with almost 1000 m^2/g and a high O/C ratio of 0.66. However, this latter data would strongly indicate that although porosity and oxygen surface groups benefit CWAO, the high loading of metallic species plays a crucial role in the catalytic performance of the materials prepared in this work.

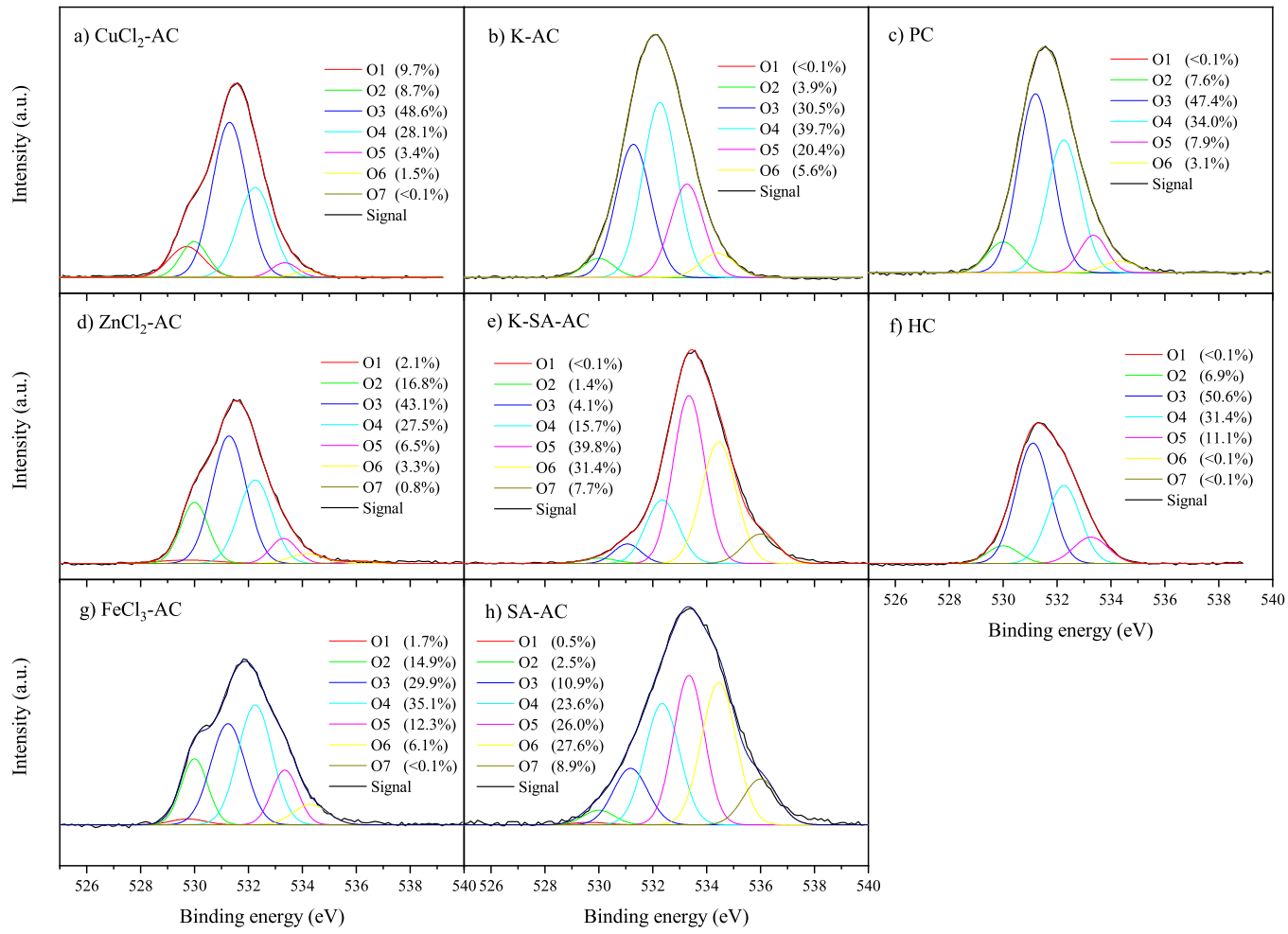

Fig. 3. XPS deconvolution fit.

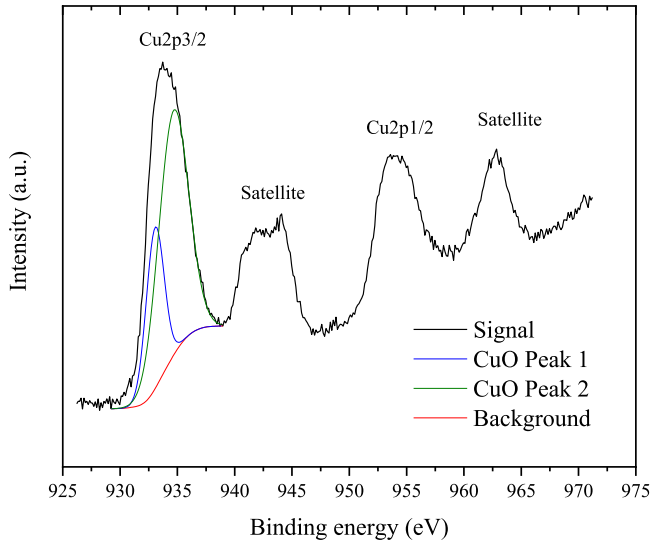

Fig. 4. XPS deconvolution fit of $CuCl_2$–AC catalyst.

Concerning the works reported in the literature, impressive results of iron and copper catalysts were obtained for wet air oxidation of real pharmaceutical [18] and petroleum refining [58] wastewaters, achieving up to 95% and 87% of TOC removals, respectively. However, these catalysts were not carbon-based materials and did not involve the utilization of waste materials. On the other hand, more examples can be found in literature focused on the catalytic performance of numerous materials but using model pollutants. In this sense, for instance, a copper oxide-loaded activated carbon catalyst achieved complete dye decolorization (100%) and an 88% COD conversion for CWAO of an azo dye compound [59]. Additionally, Gutiérrez-Sánchez et al. investigated the degradation of ciprofloxacin using an iron/activated carbon (Fe/AC) catalyst derived from pyrolysis of sludge with almost complete antibiotic removal after 2 h and achieving a 70% TOC conversion [31]. Other authors have also noted the significance of iron in WAO processes, reporting COD degradations ranging from 61% to 96% for model compounds such as glyphosate, methyl orange, and various other dyes [60, 61]. While these previous studies have reported the potential of Fe or Cu

Table 5
Actual HTC liquor characterization.

Parameter	Value
COD_t(g/L)	9.9 ± 0.6
TS (g/L)	2.2 ± 0.3
VTS (g/L)	1.4 ± 0.2
TSS (g/L)	0.60 ± 0.02
VSS (g/L)	0.46 ± 0.01
COD_s (g/L)	7.4 ± 0.2
TOC (g/L)	2.4 ± 0.3
pH	7.8 ± 0.1
PO_4^{3-} (mg/L)	80 ± 2
NH_4^+ (mg/L)	118 ± 2
TKN (mg/L)	505 ± 50

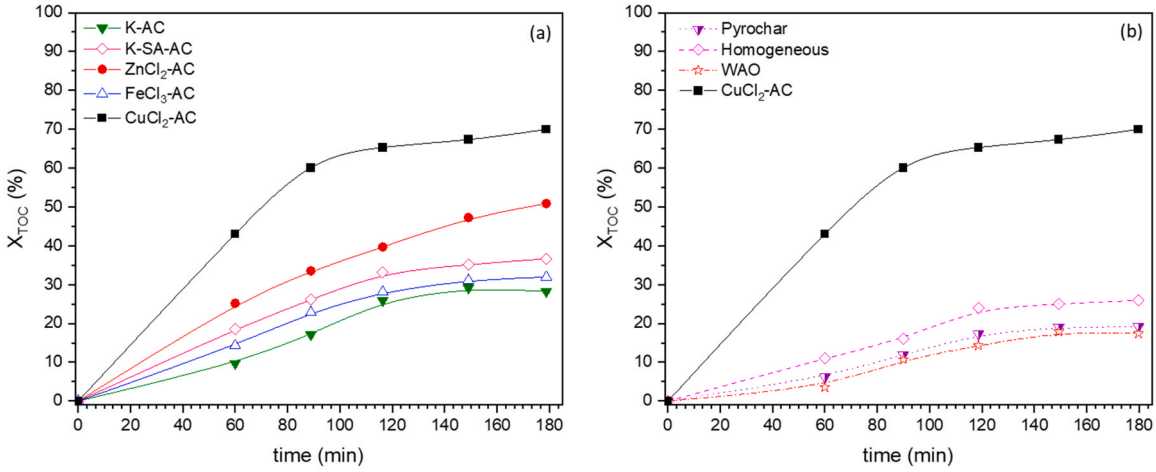

Fig. 5. TOC removal of different activated hydrochar (a) and blank reactions (b).

catalysts to enhance the performance of WAO processes, the present work explores the application of carbon-based catalysts derived from hydrochar materials produced from waste feedstocks, avoiding the use of costly synthesized catalysts, and the treatment of potential hazard aqueous streams for valorization in subsequent processes instead degradation.

Regarding the catalyst activated with KOH, the critical role of the specific surface area can be seen, as higher activity was obtained for the K-SA-AC catalyst with almost 1000 m^2/g. However, this latter data would strongly indicate that although porosity is essential, high loading of metallic species plays a crucial role in the catalytic performance of the materials prepared in this work. The stability of a catalyst is the most important parameter for evaluating whether its practical application is economically feasible. The hydrothermal stability of the catalytic materials for the CWAO of an HTC effluent was assessed in terms of the metal leaching. The amount of metal leached out from the catalyst was negligible (below the detection limit) for all the metals except for the copper in the $CuCl_2$-AC metal-doped material, where 1.17 mg/L of copper was leached out. Most authors justified the metal leaching due to an integrated effect of the pH and the reaction temperature [59]. Despite the high temperature used in this work (250 °C), the pH of the treated effluent was in the range of 6.2–6.8 in all the cases, so the catalyst would be more stable under these conditions. It is noteworthy that there are very few studies regarding the application of WAO for HTC liquor. Still, the study of Reza et al. determined that WAO in the presence of CuO may not be feasible for sludge-derived HTC process liquid [6]. Other studies on individual compounds with heterogeneous-based catalysts have shown considerable copper loss during testing (~60%) [62–64]. So, it is essential to emphasize the high stability of the copper hydrochar-based catalyst.

However, the copper leached from the catalyst could be active in a homogeneous CWAO process. Thus, a homogeneous reaction using 1.5 mg/L of Cu^{2+} ($CuCl_2$) was carried out, and the results with other blank reactions (WAO and CWAO with the pyrochar) are shown in Fig. 5b. In all cases, the degradation rates are significantly slower than that obtained for the CWAO process with the activated hydrochar. WAO, the homogeneous reaction with Cu^{2+} and the CWAO with the pyrochar show all similar values for TOC removal of ca. 22%, confirming the outstanding activity of the $CuCl_2$-AC derived hydrochar material for treating the HTC effluent. The low removal of TOC using pyrochar should be attributed to its low porosity and absence of active metal species. In all the studied cases, the physical appearance of WAO effluents is much more transparent than the HTC process liquid, although it still contains a fair amount of TOC. Thus, the color number was evaluated for each WAO effluent. High removal values were obtained between 93.8% and 99.3% for the WAO and CWAO using $CuCl_2$-CWAO experiments, respectively. This color difference indicates that the products formed during the reaction differ from the initial HTC liquor.

Fig. 6 and Tables S2 and S3 show the product distribution obtained by GC×GC-TOFMS of the initial effluent and those obtained in the CWAO process with the most active catalysts ($CuCl_2$-AC and $ZnCl_2$-AC) compared with the WAO.

Up to 97 compounds identified in the initial HTC liquor were grouped into different chemical families, such as organic acids, ketones, alcohols, phenols, aromatics, olefins and others [6]. The relative distribution of these identified compounds showed a dominance of organic acids such as acetic acid, propanoic acid, pentanoic acid or cyclohexane carboxylic acid (ca. 40%), followed by ketones (23%), phenol and derivatives (9.2%), aromatics (1.5%) and olefins (0.8%). Nitrogenous compounds such as pyrazine and pyridine derivatives were also identified, which are considered one of the main toxic compounds of the HTC liquor, along with phenol compounds and some ketones [65].

WAO and CWAO processes produce the mineralization of the organic matter to CO_2 and H_2O, as well as other oxygenated by-products such as alcohols, aldehydes, ketones, and carboxylic acids resulting from the oxidation process. Acetic acid is often one of the more refractory acid compounds that remain in higher concentration as an end by-product after WAO and CWAO treatments. A general pathway of the conversion of organic compounds into CO_2 and H_2O through wet air oxidation reactions is illustrated in Fig. 7 [53]. The distribution of final oxygenated by-products strongly depends on the oxidation conditions (temperature and pressure) and catalytic performance in the case of CWAO [66].

As shown in Fig. 6, relevant changes are observed for the treated WAO and CWAO samples. Concerning the number of the compounds initially identified in the original HTC aqueous liquor, both WAO and CWAO treatments showed a significant decrease (26, 21 and 6 for WAO, CWAO-AC-$CuCl_2$ and CWAO-AC-$ZnCl_2$ experiments, respectively). Moreover, phenolic compounds, ketones, aromatics and olefins significantly decreased or completely disappeared for the WAO and CWAO experiments. The presence of ketones and pyrazine derivatives in the WAO sample was still significant. Pyrazine derivatives were also detected for the CWAO experiment with $CuCl_2$-AC catalyst. The organic acids also decreased after WAO and CWAO treatments. These become the dominant family of by-products, particularly for CWAO experiments, considering all the identified compounds with an overall contribution of ca. 47.3%, 80.5% and 77.2% for WAO, CWAO-AC-$CuCl_2$ and CWAO-AC-$ZnCl_2$, respectively. Additionally, it must be pointed out that acetic acid was the most abundant organic acid among the detected acids. Remarkably, few compounds were found when using the $ZnCl_2$-AC catalyst compared to the $CuCl_2$-AC catalyst. This observation was made considering the outcomes of TOC removal, in which the $CuCl_2$-AC

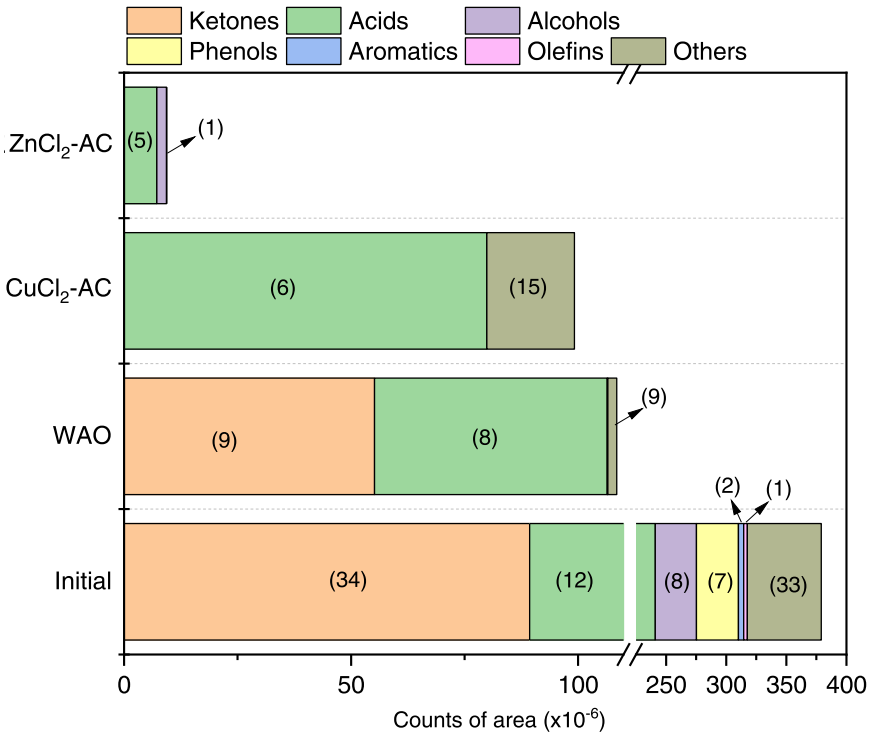

Fig. 6. Product distribution of the initial effluent, WAO and CWAO processes with $ZnCl_2$-AC and $CuCl_2$-AC. In brackets number of detected compounds.

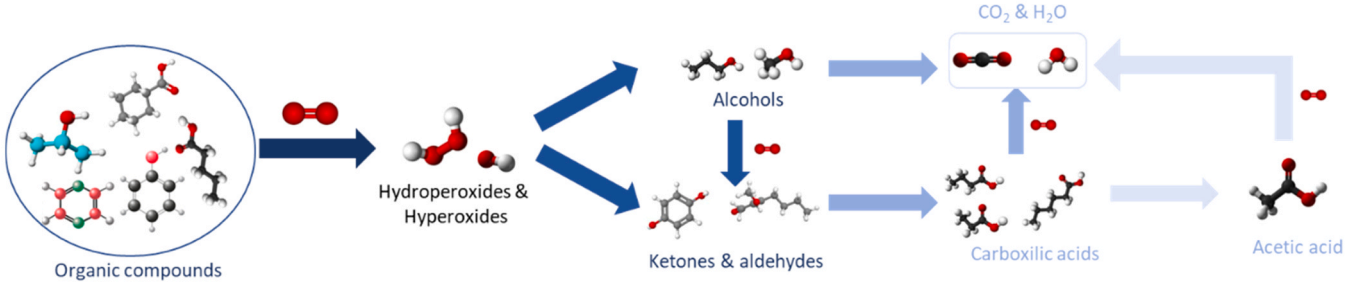

Fig. 7. General pathway for the removal of organic compounds during the WAO process.

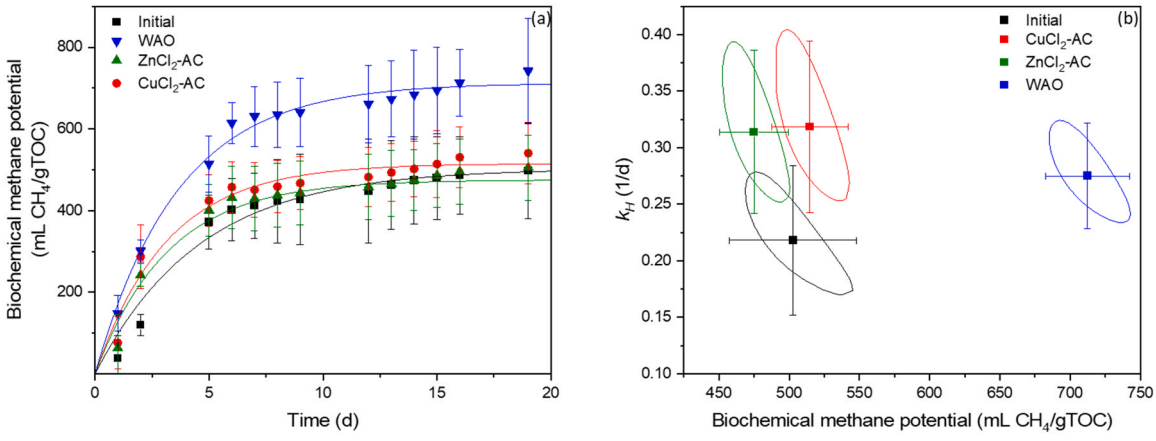

Fig. 8. Summary of the BMP tests, including the time course of the biochemical methane potential (symbols) and model fitting to the first-order model (lines) (a) and 95% confidence regions for the first-order kinetic parameters (b) for the initial effluent, WAO and CWAO processes with $ZnCl_2$-AC and $CuCl_2$-AC. All error bars indicate 95% confidence intervals from triplicates.

catalyst exhibited more significant mineralization. Consequently, conducting a more thorough examination of the resultant by-products after wet air oxidation processes is essential to uncover the compounds not being identified through the analytical technique.

It was also noteworthy that total Nitrogen (TN) was slightly reduced (2%) in the WAO process, and more significantly in the case of CWAO for the most active catalysts (9% for the $CuCl_2$-AC and 11% for the $ZnCl_2$). Potentially, this could be of concern if it indicates the production of NOx.

3.6. Biochemical methane potential (BMP) tests

Fig. 8 shows the summary of the BMP tests. Fig. 8a shows the time course of the biochemical methane potential. At first sight, the liquid sample after standard WAO achieved the highest BMP with 742 ± 129 $mLCH_4$/gTOC, corresponding to around 250 $mLCH_4$/gCOD by applying a TOC/COD ratio of 1/3. This value is relatively high compared to industrial effluents treated by WAO that yielded less than 100 $mLCH_4$/gCOD [67].

The CWAO treatments with metal-doped materials also obtained relatively high BMP values of 540 ± 75 and 505 ± 80 $mLCH_4$/gTOC for the *$CuCl_2$-AC* and *$ZnCl_2$-AC* experiments, respectively, which roughly corresponds to 180 and 168 $mLCH_4$/gCOD, respectively. In any case, the CWAO treatments seem to improve the anaerobic digestion rate, especially the treatment with $CuCl_2$-AC. As seen in Fig. 8b, the hydrolysis rate of the *$CuCl_2$-AC* and *$ZnCl_2$-AC* effluents are 1.16 and 1.14-fold the value estimated for the standard *WAO* effluent. But, the highest difference between treatments was obtained in the TOC removal. Indeed, the anaerobic digestion of the *$CuCl_2$-AC* effluent was the most effective treatment, achieving a final TOC of only 37 mgTOC/L after the anaerobic treatment. This low organic carbon content is suggested to be composed of recalcitrant organic compounds that can never be transformed. It can explain why the TOC removal efficiency of the *$CuCl_2$-AC* anaerobic treatment is slightly lower than the observed for the standard *WAO* effluent (87 vs. 95%, respectively), where the initial TOC of the *WAO* effluent was much higher than this from the *$CuCl_2$-AC* effluent (1.81 vs. 0.57 gTOC/L, respectively). As the final TOC of the *$CuCl_2$-AC* effluent is lower than that of the standard *WAO* effluent, it can be concluded that the *$CuCl_2$-AC* improved the overall biodegradability.

4. Conclusions

Hydrochar materials produced from HTC were activated using KOH, $FeCl_3$, $ZnCl_2$, and $CuCl_2$ with equal molar mass to ascertain the most effective activating agent for subsequent application as catalysts in the treatment of the HTC liquor through wet air oxidation processes. Regarding the K-SA-AC catalyst activated with KOH and washed with sulphuric acid, the highest surface area of ca. S_{BET} 1000 m^2/g was obtained. However, the activity in the CWAO was 35% of TOC conversion after 3 h. The activation with metal chlorides led to the incorporation of iron and copper into the structure of the activated metal-doped materials. The Cu-doped material with ca. 70% TOC conversion and a S_{BET} of 112 m^2/g proved to be a very efficient catalyst compared to the iron-doped material, which showed lower catalytic activity despite the high specific surface area. These results evidence that the loading of metallic species into the activated carbon materials plays a more critical role than the superficial porosity of the material in the catalytic performance. Moreover, the high stability of the hydrochar-based catalysts synthesized in this study should be underlined. On the other hand, WAO and CWAO enhance the rate of anaerobic digestion. This fact is attributed to the increase of biodegradable carboxylic acids as end by-products as well as the decrease of more toxic compounds of the HTC liquor such as ketones, phenols, aromatics, or nitrogenous pyrazine and pyridine derivatives. The effluent coming from the treatment of the $CuCl_2$-AC catalyst achieved the lowest final TOC concentration after the biochemical methane tests.

CRediT authorship contribution statement

Alberto de Mora: Validation, Investigation, Formal Analysis, Writing - Review & Editing. **José Luis Díaz de Tuesta:** Writing- Original draft, Validation, Investigation, Writing- Original draft, Formal Analysis, Writing - Review & Editing. **M. Isabel Pariente:** Writing- Original draft, Formal Analysis, Data Curation, Supervision, Validation, Writing - Review & Editing. **Yolanda Segura:** Validation, Investigation, Formal Analysis, Writing - Review & Editing, Supervision. **Daniel Puyol:** Investigation, Formal Analysis. **Estibaliz Castillo:** Investigation. **Kristina Lissitsyna:** Investigation. **Juan Antonio Melero:** Funding acquisition, Supervision. **Fernando Martínez:** Conceptualization, Methodology, Formal Analysis, Writing - Review & Editing, Project administration, Funding acquisition, Supervision.

Declaration of Competing Interest

The authors declare that they have no known competing financial interests or personal relationships that could have appeared to influence the work reported in this paper.

Data Availability

Data will be made available on request.

Acknowledgements

The authors gratefully acknowledge the financial support through the projects [PLEC2021–007761; PID2021–122883OB-I00 and TED2021–129595B-I00] funded by MCIN/AEI /10.13039/501100011033 / FEDER, UE and European Union "NextGenerationEU"/PRTR"; and [2022/00156/021] funded by Comunidad de Madrid. Jose L. Diaz De Tuesta acknowledges the financial support through the program of *Atracción al Talento* of *Comunidad de Madrid* (Spain) for the individual research grant 2022-T1/AMB-23946.

Appendix A. Supporting information

Supplementary data associated with this article can be found in the online version at doi:10.1016/j.cattod.2023.114462.

References

[1] J.L. Diaz De Tuesta, M.C. Saviotti, F.F. Roman, G.F. Pantuzza, H.J.F. Sartori, A. Shinibekova, M.S. Kalmakhanova, B.K. Massalimova, J.M.T.A. Pietrobelli, G. G. Lenzi, H.T. Gomes, Assisted hydrothermal carbonization of agroindustrial byproducts as effective step in the production of activated carbon catalysts for wet peroxide oxidation of micro-pollutants, J. Environ. Chem. Eng. 9 (2021), 105004, https://doi.org/10.1016/J.JECE.2020.105004.

[2] F.F. Roman, J.L. Diaz De Tuesta, P. Praça, A.M.T. Silva, J.L. Faria, H.T. Gomes, Hydrochars from compost derived from municipal solid waste: production process optimization and catalytic applications, J. Environ. Chem. Eng. 9 (2021), 104888, https://doi.org/10.1016/J.JECE.2020.104888.

[3] S. Masoumi, V.B. Borugadda, S. Nanda, A.K. Dalai, Hydrochar: a review on its production technologies and applications, Catalysts (2021), https://doi.org/10.3390/catal11080939.

[4] L. Leng, W. Zhou, Chemical compositions and wastewater properties of aqueous phase (wastewater) produced from the hydrothermal treatment of wet biomass: a review, Energy Sources, Part A Recover. Util. Environ. Eff. (2018), https://doi.org/10.1080/15567036.2018.1495780.

[5] R. Wang, P. Peng, S. Qi, G. Song, Z. Zhao, Q. Yin, Chemical modification of straw hydrochar as additive to improve the anaerobic digestion performance of sludge hydrothermal carbonization wastewater, Fuel 340 (2023), 127506, https://doi.org/10.1016/J.FUEL.2023.127506.

[6] M.T. Reza, A. Freitas, X. Yang, C.J. Coronella, Wet air oxidation of hydrothermal carbonization (HTC) process liquid, ACS Sustain. Chem. Eng. (2016), https://doi.org/10.1021/acssuschemeng.6b00292.

[7] L. Liu, Y. Zhai, H. Wang, X. Liu, X. Liu, Z. Wang, Y. Zhou, Y. Zhu, M. Xu, Treatment of sewage sludge hydrothermal carbonization aqueous phase by Fe(II)/CaO2 system: oxidation behaviors and mechanism of organic compounds, Waste Manag 158 (2023) 164–175, https://doi.org/10.1016/J.WASMAN.2023.01.016.

[8] Z.X. Xu, X.Q. Ma, J. Zhou, P.G. Duan, W.Y. Zhou, A. Ahmad, R. Luque, The influence of key reactions during hydrothermal carbonization of sewage sludge on

aqueous phase properties: a review, J. Anal. Appl. Pyrolysis 167 (2022), 105678, https://doi.org/10.1016/J.JAAP.2022.105678.
[9] K. Czerwińska, A. Marszałek, E. Kudlek, M. Śliz, M. Dudziak, M. Wilk, The treatment of post-processing liquid from the hydrothermal carbonization of sewage sludge, Sci. Total Environ. 885 (2023), 163858, https://doi.org/10.1016/J.SCITOTENV.2023.163858.
[10] S. Mahata, S.R. Periyavaram, N.K. Akkupalli, S. Srivastava, C. Matli, A review on Co-hydrothermal carbonization of sludge: effect of process parameters, reaction pathway, and pollutant transport, J. Energy Inst. 110 (2023), 101340, https://doi.org/10.1016/J.JOEI.2023.101340.
[11] A.I. Abd-Elhamid, M. Emran, M.H. El-Sadek, A.A. El-Shanshory, H.M.A. Soliman, M.A. Akl, M. Rashad, Enhanced removal of cationic dye by eco-friendly activated biochar derived from rice straw, Appl. Water Sci. (2020), https://doi.org/10.1007/s13201-019-1128-0.
[12] P.J. Arauzo, M.P. Olszewski, X. Wang, J. Pfersich, V. Sebastian, J. Manyà, N. Hedin, A. Kruse, Assessment of the effects of process water recirculation on the surface chemistry and morphology of hydrochar, Renew. Energy (2020), https://doi.org/10.1016/j.renene.2020.04.050.
[13] J.A. Villamil, A.F. Mohedano, J.J. Rodriguez, M.A. de la Rubia, Valorisation of the liquid fraction from hydrothermal carbonisation of sewage sludge by anaerobic digestion, J. Chem. Technol. Biotechnol. (2018), https://doi.org/10.1002/jctb.5375.
[14] L.P. Xiao, Z.J. Shi, F. Xu, R.C. Sun, Hydrothermal carbonization of lignocellulosic biomass, Bioresour. Technol. (2012), https://doi.org/10.1016/j.biortech.2012.05.060.
[15] M.T. Reza, C. Coronella, K.M. Holtman, D. Franqui-Villanueva, S.R. Poulson, Hydrothermal carbonization of autoclaved municipal solid waste pulp and anaerobically treated pulp digestate, ACS Sustain. Chem. Eng. (2016), https://doi.org/10.1021/acssuschemeng.6b00160.
[16] J. Levec, A. Pintar, Catalytic wet-air oxidation processes: a review, Catal. Today (2007), https://doi.org/10.1016/j.cattod.2007.03.035.
[17] M. Wilk, K. Czerwińska, M. Śliz, M. Imbierowicz, Hydrothermal carbonization of sewage sludge: Hydrochar properties and processing water treatment by distillation and wet oxidation, Energy Rep. 9 (2023) 39–58, https://doi.org/10.1016/J.EGYR.2023.03.092.
[18] Ö. Berkün Olgun, B. Palas, S. Atalay, G. Ersöz, Photocatalytic oxidation and catalytic wet air oxidation of real pharmaceutical wastewater in the presence of Fe and LaFeO3 doped activated carbon catalysts, Chem. Eng. Res. Des. 171 (2021) 421–432, https://doi.org/10.1016/J.CHERD.2021.05.017.
[19] H. Shan, R. Oh, J. Fan, X. Zhang, N. Zhang, X. Huang, G.-S. Park, Q. Zheng, H. Lu, B. Chen, Developing Pt-M/C catalyst (M=Pb, Cu) for efficient catalytic wet air oxidation of phenol wastewater under mild conditions, J. Environ. Chem. Eng. 11 (2023), 109854, https://doi.org/10.1016/J.JECE.2023.109854.
[20] Z. Jiang, Y. Xie, C. Li, J. Zheng, M. Si, R. Xiao, Q. Liao, W. Yang, Non-radical dominated catalytic degradation of chlorophenol by a structure-tailored catalyst of high nitrogen doping carbon matrix with nano-CuO, SSRN Electron. J. (2022), https://doi.org/10.2139/ssrn.3989903.
[21] B. Feng, L. Hao, C. Deng, J. Wang, H. Song, M. Xiao, T. Huang, Q. Zhu, H. Gai, A highly hydrothermal stable copper-based catalyst for catalytic wet air oxidation of m-cresol in coal chemical wastewater, Chin. J. Chem. Eng. 57 (2023) 338–348, https://doi.org/10.1016/J.CJCHE.2022.11.006.
[22] S. Keav, J. Barbier, D. Duprez, Deactivation and regeneration of wet air oxidation catalysts, Catal. Sci. Technol. (2011), https://doi.org/10.1039/c0cy00085j.
[23] R.P. Rocha, M.F.R. Pereira, J.L. Figueiredo, Metal-free carbon materials as catalysts for wet air oxidation, Catal. Today 356 (2020) 189–196, https://doi.org/10.1016/j.cattod.2019.04.047.
[24] J.L. Diaz De Tuesta, F.F. Roman, V.C. Marques, A.S. Silva, A.P.F. Silva, T.C. Bosco, A.A. Shinibekova, S. Aknur, M.S. Kalmakhanova, B.K. Massalimova, M. Arrobas, A. M.T. Silva, H.T. Gomes, Performance and modeling of Ni(II) adsorption from low concentrated wastewater on carbon microspheres prepared from tangerine peels by FeCl3-assisted hydrothermal carbonization, J. Environ. Chem. Eng. (2022), https://doi.org/10.1016/j.jece.2022.108143.
[25] J. Wang, T.L. Liu, Q.X. Huang, Z.Y. Ma, Y. Chi, J.H. Yan, Production and characterization of high quality activated carbon from oily sludge, Fuel Process. Technol. (2017), https://doi.org/10.1016/j.fuproc.2017.03.017.
[26] S. Brunauer, P.H. Emmett, E. Teller, Adsorption of gases in multimolecular layers, J. Am. Chem. Soc. (1938), https://doi.org/10.1021/ja01269a023.
[27] B.C. Lippens, J.H. de Boer, Studies on pore systems in catalysts. V. The t method, J. Catal. (1965), https://doi.org/10.1016/0021-9517(65)90307-6.
[28] J.L. Diaz de Tuesta, A.M.T. Silva, J.L. Faria, H.T. Gomes, Removal of Sudan IV from a simulated biphasic oily wastewater by using lipophilic carbon adsorbents, Chem. Eng. J. 347 (2018) 963–971, https://doi.org/10.1016/J.CEJ.2018.04.105.
[29] C. González, M.I. Pariente, R. Molina, L.G. Espina, M.O. Masa, V. Bernal, J. A. Melero, F. Martínez, Increasing biodegradability of a real amine-contaminated spent caustic problematic stream through WAO and CWAO oxidation using a high specific surface catalyst from petcoke, Chem. Eng. J. (2023), https://doi.org/10.1016/j.cej.2023.141692.
[30] P. Wang, Y.N. Liang, Z. Zhong, X. Hu, Nano-hybrid bimetallic Au-Pd catalysts for ambient condition-catalytic wet air oxidation (AC-CWAO) of organic dyes, Sep. Purif. Technol. 233 (2020), 115960, https://doi.org/10.1016/J.SEPPUR.2019.115960.
[31] P. Gutiérrez-Sánchez, S. Álvarez-Torrellas, M. Larriba, M.V. Gil, J.M. Garrido-Zoido, J. García, Efficient removal of antibiotic ciprofloxacin by catalytic wet air oxidation using sewage sludge-based catalysts: Degradation mechanism by DFT studies, J. Environ. Chem. Eng. 11 (2023), 109344, https://doi.org/10.1016/J.JECE.2023.109344.
[32] G. de Freitas Batista, F.F. Roman, J.L.D. de Tuesta, R.V. Mambrini, P. Praça, H. T. Gomes, Assessment of pretreatments for highly concentrated leachate waters to enhance the performance of catalytic wet peroxide oxidation with sustainable low-cost catalysts, Catalysts (2022), https://doi.org/10.3390/catal12020238.
[33] C. Tizaoui, L. Bouselmi, L. Mansouri, A. Ghrabi, Landfill leachate treatment with ozone and ozone/hydrogen peroxide systems, J. Hazard. Mater. (2007), https://doi.org/10.1016/j.jhazmat.2006.09.023.
[34] D. Puyol, A.F. Mohedano, J.J. Rodriguez, J.L. Sanz, Effect of 2,4,6-trichlorophenol on the microbial activity of adapted anaerobic granular sludge bioaugmented with Desulfitobacterium strains, N. Biotechnol. (2011), https://doi.org/10.1016/j.nbt.2011.06.011.
[35] Y. Segura, R. Molina, I. Rodríguez, T. Hülsen, D. Batstone, V. Monsalvo, F. Martínez, J.A. Melero, D. Puyol, Improvement of biogas production and nitrogen recovery in anaerobic digestion of purple phototrophic bacteria by thermal hydrolysis, Bioresour. Technol. (2023), https://doi.org/10.1016/j.biortech.2022.128250.
[36] I. de las Heras, R. Molina, Y. Segura, T. Hülsen, M.C. Molina, N. Gonzalez-Benítez, J.A. Melero, A.F. Mohedano, F. Martínez, D. Puyol, Contamination of N-poor wastewater with emerging pollutants does not affect the performance of purple phototrophic bacteria and the subsequent resource recovery potential, J. Hazard. Mater. 385 (2020), 121617, https://doi.org/10.1016/j.jhazmat.2019.121617.
[37] D.J. Batstone, P.F. Pind, I. Angelidaki, Kinetics of thermophilic, anaerobic oxidation of straight and branched chain butyrate and valerate, Biotechnol. Bioeng. (2003), https://doi.org/10.1002/bit.10753.
[38] L.S.K. Pang, J.D. Saxby, S.P. Chatfield, Thermogravimetric analysis of carbon nanotubes and nanoparticles, J. Phys. Chem. (1993), https://doi.org/10.1021/j100129a001.
[39] M. Heidari, O. Norouzi, K. MacDermid-Watts, B. Acharya, Y. Zhang, A. Dutta, Product evaluation of hydrothermal carbonization of biomass: semi-continuous vs. batch feeding, Biomass-.-. Convers. Biorefinery. (2022), https://doi.org/10.1007/s13399-020-00932-6.
[40] J.L. Diaz de Tuesta, G. F. Pantuzza, A.M.T. Silva, P. Praça, J.L. Faria, H.T. Gomes, Catalysts prepared with matured compost derived from mechanical-biological treatment plants for the wet peroxide oxidation of pollutants with different lipophilicity, Catalysts (2020), https://doi.org/10.3390/catal10111243.
[41] J.L. Diaz de Tuesta, F.V.M. de Almeida, J.R.P. Oliveira, P. Praça, M.C. Guerreiro, H. T. Gomes, Kinetic insights on wet peroxide oxidation of caffeine using EDTA-functionalized low-cost catalysts prepared from compost generated in municipal solid waste treatment facilities, Environ. Technol. Innov. (2021), https://doi.org/10.1016/j.eti.2021.101984.
[42] E. Erdogan, B. Atila, J. Mumme, M.T. Reza, A. Toptas, M. Elibol, J. Yanik, Characterization of products from hydrothermal carbonization of orange pomace including anaerobic digestibility of process liquor, Bioresour. Technol. 196 (2015) 35–42, https://doi.org/10.1016/J.BIORTECH.2015.06.115.
[43] E.M. Cepollaro, D. Caputo, S. Cimino, N. Gargiulo, L. Lisi, Synthesis and Characterization of Activated Carbon Foam from Polymerization of Furfuryl Alcohol Activated by Zinc and Copper Chlorides, C. — J. Carbon Res (2020), https://doi.org/10.3390/c6030045.
[44] P. Lawtae, C. Tangsathitkulchai, A new approach for controlling mesoporosity in activated carbon by the consecutive process of air oxidation, thermal destruction of surface functional groups, and carbon activation (The OTA method), Molecules (2021), https://doi.org/10.3390/molecules26092758.
[45] F. Heras, N. Alonso-Morales, D. Jimenez-Cordero, M.A. Gilarranz, J.J. Rodriguez, Granular mesoporous activated carbons from waste tires by cyclic oxygen chemisorption-desorption, Ind. Eng. Chem. Res. (2012), https://doi.org/10.1021/ie201499h.
[46] J.L. Diaz de Tuesta, A. Quintanilla, J.A. Casas, J.J. Rodriguez, P-, B- and N-doped carbon black for the catalytic wet peroxide oxidation of phenol: activity, stability and kinetic studies, Catal. Commun. (2017), https://doi.org/10.1016/j.catcom.2017.09.012.
[47] J.J. Pireaux, High resolution XPS of organic polymers: the scienta ESCA300 database, J. Electron Spectros. Relat. Phenom. (1993), https://doi.org/10.1016/0368-2048(93)85006-7.
[48] M.C. Biesinger, L.W.M. Lau, A.R. Gerson, R.S.C. Smart, Resolving surface chemical states in XPS analysis of first row transition metals, oxides and hydroxides: Sc, Ti, V, Cu and Zn, Appl. Surf. Sci. (2010), https://doi.org/10.1016/j.apsusc.2010.07.086.
[49] M.C. Biesinger, Advanced analysis of copper X-ray photoelectron spectra, Surf. Interface Anal. (2017), https://doi.org/10.1002/sia.6239.
[50] P.L. Qin, H.W. Lei, X.L. Zheng, Q. Liu, H. Tao, G. Yang, W.J. Ke, L. Bin Xiong, M. C. Qin, X.Z. Zhao, G.J. Fang, Copper-doped chromium oxide hole-transporting layer for perovskite solar cells: interface engineering and performance improvement, Adv. Mater. Interfaces (2016), https://doi.org/10.1002/admi.201500799.
[51] M. Mantovani, E. Collina, F. Marazzi, M. Lasagni, V. Mezzanotte, Microalgal treatment of the effluent from the hydrothermal carbonization of microalgal biomass, J. Water Process Eng. (2022), https://doi.org/10.1016/j.jwpe.2022.102976.
[52] M. Usman, H. Chen, K. Chen, S. Ren, J.H. Clark, J. Fan, G. Luo, S. Zhang, Characterization and utilization of aqueous products from hydrothermal conversion of biomass for bio-oil and hydro-char production: a review, Green. Chem. (2019), https://doi.org/10.1039/c8gc03957g.
[53] H. Debellefontaine, J.N. Foussard, Wet air oxidation for the treatment of industrial wastes. Chemical aspects, reactor design and industrial applications in Europe, Waste Manag (2000), https://doi.org/10.1016/S0956-053X(99)00306-2.

[54] R.P. Rocha, M.F.R. Pereira, J.L. Figueiredo, Metal-free carbon materials as catalysts for wet air oxidation, Catal. Today (2020), https://doi.org/10.1016/j.cattod.2019.04.047.
[55] T. Wakabayashi, A. Okuwaki, Oxidation of coals in liquid phases. IX. Kinetics of the base-catalyzed oxidation of acetate ion by oxygen at elevated temperatures, Bull. Chem. Soc. Jpn. (1988), https://doi.org/10.1246/bcsj.61.4329.
[56] J. Tardio, S. Bhargava, S. Eyer, M. Sumich, D.B. Akolekar, Interactions between specific organic compounds during catalytic wet oxidation of bayer liquor, Ind. Eng. Chem. Res. (2004), https://doi.org/10.1021/ie030539g.
[57] J. Wang, W. Fu, X. He, S. Yang, W. Zhu, Catalytic wet air oxidation of phenol with functionalized carbon materials as catalysts: reaction mechanism and pathway, J. Environ. Sci. (China). (2014), https://doi.org/10.1016/j.jes.2014.06.015.
[58] W. Ma, S. Zhang, L. Deng, D. Zhong, K. Li, X. Liu, J. Li, J. Zhang, J. Ma, Cu-based perovskite as a novel CWPO catalyst for petroleum refining wastewater treatment: performance, toxicity and mechanism, J. Hazard. Mater. 448 (2023), 130824, https://doi.org/10.1016/j.jhazmat.2023.130824.
[59] B. Ayalkie Gizaw, N. Gabbiye Habtu, Catalytic wet air oxidation of azo dye (reactive red 2) over copper oxide loaded activated carbon catalyst, J. Water Process Eng. 48 (2022), 102797, https://doi.org/10.1016/J.JWPE.2022.102797.
[60] P. Gupta, N. Verma, Evaluation of degradation and mineralization of glyphosate pollutant in wastewater using catalytic wet air oxidation over Fe-dispersed carbon nanofibrous beads, Chem. Eng. J. 417 (2021), https://doi.org/10.1016/j.cej.2020.128029.
[61] J. Fu, G.Z. Kyzas, Wet air oxidation for the decolorization of dye wastewater: an overview of the last two decades, Chin. J. Catal. 35 (2014) 1–7, https://doi.org/10.1016/S1872-2067(12)60724-4.
[62] Q. Wu, X. Hu, P.L. Yue, X.S. Zhao, G.Q. Lu, Copper/MCM-41 as catalyst for the wet oxidation of phenol, Appl. Catal. B Environ. (2001), https://doi.org/10.1016/S0926-3373(01)00131-X.
[63] S. Hočevar, U.O. Krašovec, B. Orel, A.S. Aricó, H. Kim, CWO of phenol on two differently prepared CuO-CeO2 catalysts, Appl. Catal. B Environ. (2000), https://doi.org/10.1016/S0926-3373(00)00167-3.
[64] A.M.T. Silva, R.M. Quinta-Ferreira, J. Levec, Catalytic and noncatalytic wet oxidation of formaldehyde. A novel kinetic model, Ind. Eng. Chem. Res. (2003), https://doi.org/10.1021/ie030090r.
[65] M.E. Suárez-Ojeda, J. Carrera, I.S. Metcalfe, J. Font, Wet air oxidation (WAO) as a precursor to biological treatment of substituted phenols: refractory nature of the WAO intermediates, Chem. Eng. J. (2008), https://doi.org/10.1016/j.cej.2008.01.022.
[66] W. Sun, H. Wu, C. Jin, P. Han, M. Liu, H. Wei, C. Sun, The effect of different inorganic anions on mineralization of acrylic acid in wet air oxidation, Chemosphere (2020), https://doi.org/10.1016/j.chemosphere.2019.125463.
[67] T. Sarat Chandra, S.N. Malik, G. Suvidha, M.L. Padmere, P. Shanmugam, S. N. Mudliar, Wet air oxidation pretreatment of biomethanated distillery effluent: mapping pretreatment efficiency in terms color, toxicity reduction and biogas generation, Bioresour. Technol. (2014), https://doi.org/10.1016/j.biortech.2014.01.106.